Int. J. Nonlinear Anal. Appl. 13 (2022) 2, 499–513
ISSN: 2008-6822 (electronic)
http://dx.doi.org/10.22075/ijnaa.2021.24232.2700

An iterative algorithm for nonlinear fractional-order oscillators with modified Riemann-Liouville derivative

Akuro Big-Alabo, Chinwuba Victor Ossia*

Applied Mechanics and Design (AMD) Research Group, Department of Mechanical Engineering, Faculty of Engineering, University of Port Harcourt, Port Harcourt, Nigeria

(Communicated by Madjid Eshaghi Gordji)

Abstract

This paper presents an iterative analytic algorithm for the approximate solution of nonlinear fractional-order oscillators. The He fractional transform was applied to convert the fractional-order model, defined by a modified Riemann-Liouville derivative, to a model in continuous spacetime. Then, the approximate solution of the continuous model was applied to obtain an approximate solution for the fractional-order oscillator. The solution was obtained using the continuous piecewise linearization method (CPLM), which is a simple, accurate and efficient analytic algorithm. The applicability of the CPLM was demonstrated using representative examples in science and engineering and the maximum relative error of the approximate solution was found to be less than 0.2 per cent. This paper provides an analytical tool that can be applied in the study of fractional-order oscillations arising in various physical systems and technological processes.

Keywords: continuous piecewise linearization method, nonlinear oscillation, fractional-order oscillator, fractional spacetime, Riemann-Liouville derivative, He fractional transform
2020 MSC: Primary 26A33, 34C15, 37M15; Secondary 37N05, 37N15, 37N20, 37J65, 37C60

1 Introduction

The concept of fractional derivative was invented about the same time with integer-order derivative but while the latter witnessed significant mathematically developments due to the understanding of its immediate physical relevance, the former had to wait until several decades due to its lack of apparent physical application. In recent times, many applications of fractional derivatives have been found and this has sparked renewed interest in the subject. Examples of application of fractional derivatives include flow in porous media [14], quantum mechanics [19, 17], heat conduction [33], solitary motion in shallow water [31], anomalous diffusion [26], relaxation systems [12], visco-elastic materials with memory effect [11], biological material transport [29] and fractional oscillators [13, 30]. A lucid and comprehensive account of the historical developments in the definition and characterization of fractional derivatives can be found in ref. [32]. Of the several definitions of fractional derivatives, the most common definitions are the Riemann-Liouville

*Corresponding author
Email addresses: akuro.big-alabo@uniport.edu.ng (Akuro Big-Alabo), chinwuba.ossia@uniport.edu.ng (Chinwuba Victor Ossia)

Received: July 2021 *Accepted:* August 2021

(R-L) and Caputo fractional derivatives given by equations (1) and (2) respectively,

$$ {}^{RL}{}_0D_t^{\alpha} = \frac{1}{\Gamma(n-\alpha)} \frac{d^n}{d\tau^n} \int_0^t (t-\tau)^{n-\alpha-1} x(\tau) d\tau \tag{1.1} $$

$$ {}^{C}{}_0D_t^{\alpha} = \frac{1}{\Gamma(n-\alpha)} \int_0^t (t-\tau)^{n-\alpha-1} x^n(\tau) d\tau \tag{1.2} $$

where $n-1 < \alpha < n$, $\alpha > 0$, $n >= 1$, $x^n(\tau) = d^n x/d\tau^n$ and $\Gamma(x)$ is the gamma function of x. These definitions have their limitations. For instance, the R-L derivative requires initial conditions in terms of non-integer derivatives which lack any physical interpretation. Also, when the R-L derivative is applied to a constant, it produces another constant instead of zero as with integer-order derivative. The Caputo derivative overcomes both of these challenges and is mostly used to analyze physical problems [1]. However, the Caputo derivative requires that the function to which it is applied must be continuous and differentiable. Hence, it cannot be applied to discontinuous spacetime systems such as porous media and hierarchical structures. Furthermore, the Caputo derivative does not have an antiderivative associate in the same manner as the R-L derivative [1].

Recent definitions of fractional derivatives seek to generalize existing definitions [20, 21], capture more of the traditional properties of integer-order derivatives [22], modify existing definitions to remove restrictions [19] and provide other physically relevant applications based on nonsingular kernels [1, 10, 2]. Although these definitions are mathematically elegant, the main issue in applying them to study physical phenomena and systems lies in the solution of the resulting fractional differential equation (FDE). For linear FDEs, the solution can be readily obtained in closed-form based on the Mittag-Leffler function [13], but the same cannot be said of nonlinear FDEs. In the latter case, numerical methods or other approximate analytical methods are generally required. Atangana and Gomez-Aguilar [1] proposed a numerical scheme for the solution of FDEs based on power law, exponential decay and Mittag-Leffler kernels in the R-L sense. The numerical scheme was applied to solve the diffusion-convection equation. Atangana and Gomez-Aguilar [2] used a traditional predictor-corrector numerical scheme to investigate the solution of FDEs based on Riemann-Liouville, Caputo-Fabrizio and Atangana-Baleanu kernels. They illustrated their numerical method by solving the fractional logistic model of the Verhulst type, the fractional-order Arneodo system and the fractional-order convection-diffusion system among other FDEs. Liu et al [24] studied the nonlinear time-fractional cable equation using a two-grid finite element approximation, which is a numerical scheme. Morales-Delgado et al [29] studied oxygen transport in tissue based on Caputo and Caputo-Fabrizio fractional operators. The FDEs for the tissue oxygen transport were solved using a Laplace homotopy method, which is a combination of the Laplace transform and homotopy analysis method. He [14] studied seepage flow with fractional derivatives in porous media using the variational iteration method. The R-L fractional derivative was used to model the seepage flow in porous media. Momani and Odibat [20] used the homotopy perturbation method to solve partial differential equations of fractional order. Wang and An [30] investigated a fractional Duffing oscillator defined by He fractional derivative and has application in microphysics and tsunami motion. They applied the He fractional transform (HFT) and the amplitude-frequency method to determine the noise in the system. The HFT converts the FDE to an ODE with integer-order derivatives. In order words, the fractional complex transform converts the problem from a discontinuous (fractal) spacetime to a continuous spacetime [18]. More on the He fractional derivative and the corresponding HFT can be found in the following references [17, 18, 16].

Important features of the HFT are its physical foundation and practical relevance for investigating initial and boundary value problems [18]. This implies that the HFT can be applied to fractional oscillators with nonlinear restoring force. The purpose of this paper is to present an accurate approximate solution for solving nonlinear fractional-order oscillators using the continuous piecewise linearization method (CPLM). The fractional oscillator model was defined based on the Jumarie or modified R-L derivative and the resulting integer-order ODE obtained using the HFT was solved using the CPLM. The CPLM solution of the integer-order ODE was then applied to obtain an approximate solution for the original fractional-order model. The CPLM is an iterative algorithm that can be used to determine the periodic solution of conservative systems modeled by integer-order ODEs [3, 9]. Its attractive features are simplicity and accuracy irrespective of the complex nature of the nonlinear restoring force.

2 Modified Riemann-Liouville Derivative and He Fractional Transform

The simplest kernel used in the definition of fractional derivatives is the power-law kernel and the R-L derivative is based on this kernel. However, the use of R-L derivative to define initial value problems is limited by the fact that it is characterized by fractional-order initial conditions that make no physical sense, and that it gives a non-zero constant instead of zero when used to differentiate a constant. In order to deal with the problem of differentiation of constant,

Jumarie [19] proposed a modified R-L derivative that gives zero when it is applied to differentiate a constant and still, can be used to define systems with discontinuous spacetime. The modified R-L derivative can be derived also using the variational iteration method [17]. The modified R-L derivative or Jumarie derivative is defined as:

$$ {}^{MRL}{}_0D_t^{\alpha} = \frac{1}{\Gamma(n-\alpha)} \frac{d^n}{d\tau^n} \int_0^t (t-\tau)^{n-\alpha-1} [x(\tau) - x(0)] d\tau \tag{2.1} $$

where $x(\tau)$ is a continuous but non-differential function. Equation (2.1) obeys the following differentiation rules [17]:

$$ \frac{\partial^{\alpha} c}{\partial \tau^{\alpha}} = 0 \tag{2.2a} $$

$$ \frac{\partial^{\alpha}(cx(t))}{\partial \tau^{\alpha}} = c \frac{\partial^{\alpha} x}{\partial \tau^{\alpha}} \tag{2.2b} $$

$$ \frac{\partial^{\alpha} t^{\beta}}{\partial \tau^{\alpha}} = \frac{\Gamma(1+\beta)}{\Gamma(1+\beta-\alpha)} \tag{2.2c} $$

where c is a constant and $\beta \geq \alpha > 0$.

In spite of the success of the Jumarie derivative to deal with the problem of differentiation of a constant encountered with the classical R-L derivative, there is still the problem of fractional-order initial conditions. Based on geometrical considerations, He [15] defined a new spacetime with fractional dimensions and showed that this definition can be applied to define a fractional complex transform based on the Jumarie derivative. The fractional complex transform, called He fractional transform (HFT), eliminates the need to use fractional-order initial conditions. Hence, we explore the HFT in more details by considering a geometric perspective.

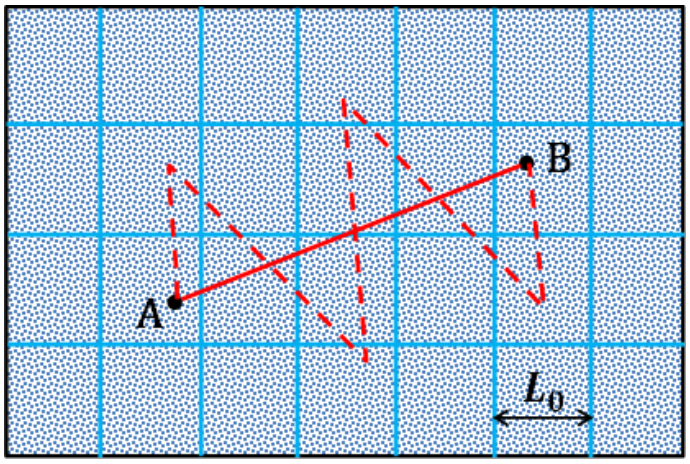

Figure 1: Particle moving from point A to B in a fractal space. Solid line represents a continuous trajectory while broken line represents the actual trajectory.

Figure 1 shows a fractal space which is a discontinuous medium. The motion of a particle in the fractal space is best described in terms of a fractional derivative. The grid in Figure 1 is rectangular and its smallest side is assumed to have a length that is greater than or equal to L_0, the smallest measure less than which any discontinuity is ignored and no physical meaning exist. In reality, L_0 can represent the nano-porous size of a porous flow medium or the diameter of a carbon nanotube. Therefore, the distance between two points A and B on the fractal space is the length of the broken zigzag line which can be defined as [18]:

$$ L_{AB} = kL_0^{\alpha} \tag{2.3} $$

where α is the fractional dimension of the fractal space and $k = k(\alpha)$ is a constant that is dependent on the fractional dimension. The estimated fractal distance L_{AB} can be viewed as a continuous variable (X) while L_0 represents the corresponding fractal variable (x). Therefore, the HFT for conversion of a fractional derivative to an integer-order derivative can be defined as [18]:

$$ X = \frac{x^{\alpha}}{\Gamma(1+\alpha)} \tag{2.4} $$

where $k(\alpha) = 1/\Gamma(1+\alpha)$. Equation (2.4) implies that $X = x$ when $\alpha = 1$, as would be expected. This geometry-based definition of a fractal space is also applicable to a fractal time dimension. Now, using equation (2.4), we can define a local fractal gradient between points A and B as shown:

$$\nabla^{\alpha} y = \frac{y_B - y_A}{L_{AB}} = \Gamma(1+\alpha) \lim_{(x_B - x_A) \to L_0} \left[\frac{y_B - y_A}{(x_B - x_A)^{\alpha}} \right] = \frac{dy}{dx^{\alpha}} \tag{2.5}$$

where y is a variable that depends on the fractal space. Equation (2.5) is a special case of a local fractional derivative that has the same properties (i.e. equations (2.2a-c)) as the Jumarie derivative and obeys simple chain rules of differentiation [17]. In order words, the HFT is a transformative approach that can convert fractional-order derivatives based on the Jumarie definition to the corresponding integer-order derivatives. This transformation process is useful for solving fractional-order oscillators because integer-order initial conditions, which have physical meaning, can be applied in the solution process. The application of the HFT and CPLM to study fractional-order nonlinear oscillators is the main objective of this article.

3 Solution methodology

We consider a general nonlinear fractional-order oscillator of the form:

$$\frac{d^2u}{dt^{2\alpha}} + f(u(t), D_t^{\alpha} u(t)) = 0 \tag{3.1}$$

with initial conditions $u(0) = A$ and $D^{\alpha}u(0) = 0$; where $D_t^{\alpha}u(t) = \frac{du}{dt^{\alpha}}$ and $f(u(t), D_t^{\alpha}u(t))$ is a general nonlinear fractional-order restoring force. The fractional derivatives in equation (3.1) are defined by equation (2.1). The HFT for equation (3.1) is given as:

$$T = \frac{t^{\alpha}}{\Gamma(1+\alpha)} \tag{3.2}$$

Transforming equation (3.1) using the HFT gives the equivalent integer-order model as [17, 30]:

$$\frac{d^2u}{dT^2} + f(u(T), u'(T)) = 0 \tag{3.3}$$

with initial conditions $u(0) = A$ and $u'(0) = 0$. Although the force in equation (3.3) is a function of $u'(T)$, dissipative forces are not considered; but rather, only even powers of $u'(T)$ (e.g. non-natural oscillators [4]) that add to the conservative restoring force are considered. Therefore, the nonlinear restoring force $f(u(T), u'(T))$ can be expressed as $f(u(T))$ using the technique in ref [4]. So, equation (3.3) can be written as:

$$\frac{d^2u}{dT^2} + f(u) = 0 \tag{3.4}$$

For simplicity $u(T)$ has been written as u. Now, equation (3.4) can be solved using the CPLM.

The CPLM is based on piecewise discretization and linearization of the nonlinear restoring force. The technique of the CPLM involves n equal discretization of the nonlinear force (i.e. $f(u)$ in this case) and formulating a linear restoring force for each discretization. Consequently, a linear ODE can be derived for each discretization. The solution to the linear ODE gives an approximate solution to the original nonlinear ODE for a range of the independent variable that is based on the range of the dependent variable (u-range) of each discretization. The range of the independent variable and the integration constants are automatically determined by the CPLM algorithm and are updated continuously from one discretization to the next. The u-range over which the discretization is done depends on the nature of the restoring force. If the restoring force is odd and symmetric, i.e. $f(\pm u) = \pm f(u)$, then the discretization is done over a quarter cycle ($0 \le u \le A$) otherwise it is done over a half cycle ($-A \le u \le A$). A detailed formulation of the CPLM algorithm can be found in the following studies [3, 9, 7] while application of the CPLM to study complex nonlinear oscillators can be found in ref [8, 6, 4].

According to the CPLM, the linearized force for each discretization can be expressed as [9]:

$$F_{rs}(u) = \pm |K_{rs}|(u - u_r) + F_r \tag{3.5}$$

where $K_{rs} = [f(u_s) - f(u_r)]/(u_s - u_r)$ is the linear slope of $F_{rs}(u)$ between points r and s, $F_r = f(u_r)$, r is the start point and s is the endpoint of each discretization. Substituting equation (3.5) in (3.4) gives the linearized equation for each discretization as follows:

$$u'' \pm |K_{rs}|u = \pm |K_{rs}|u_r - F_r \tag{3.6}$$

where the prime denotes differentiation with respect to T. The solution to equation (3.6) depends on whether the sign is positive or negative.

3.1 Solution for positive linearized stiffness

When the sign in equation (3.6) is positive the solution is:

$$u(T) = R_{rs}\sin(\omega_{rs}(T - T_r) + \Phi_{rs}) + C_{rs} \tag{3.7}$$

which can be expressed in the fractional time as:

$$u(t) = R_{rs}\sin\left(\frac{\omega_{rs}}{\Gamma(1+\alpha)}(t^\alpha - t_r^\alpha) + \Phi_{rs}\right) + C_{rs} \tag{3.8}$$

where $t_r = (T_r\Gamma(1+\alpha))^{1/\alpha}$, $\omega_{rs} = \sqrt{K_{rs}}$, $C_rs = u_r - F_r/K_{rs}$ and $R_{rs} = [(u_r - C_{rs})^2 + (u'_r/\omega_{rs})^2]^{1/2}$. The initial conditions and other parameters for each discretization are determined based on the oscillation stage. For the oscillation stage that moves from $+A$ to $-A$ the initial conditions for each discretization are $u_r = u_r(0) = A - r\Delta u$ and $u'_r = u'_r(0) = -\sqrt{|2\int_A^{u_r} -f(u)du|}$; where $\Delta u = A/n$ and the other parameters are calculated as:

$$\Phi_{rs} = \begin{cases} 0.5\pi & \text{if } u'_r = 0 \\ \pi + \tan^{-1}[\omega_{rs}(u_r - C_{rs})/u'_r] & \text{if } u'_r < 0 \end{cases} \tag{3.9}$$

and

$$\Delta T = \begin{cases} (0.5\pi - \Phi_{rs})/\omega_{rs} & \text{if } (u_s - C_{rs}) \geq R_{rs} \\ (0.5\pi + \cos^{-1}[(u_s - C_{rs})/R_{rs}] - \Phi_{rs})/\omega_{rs} & \text{if } (u_s - C_{rs}) < R_{rs} \end{cases} \tag{3.10}$$

For the oscillation stage that moves from $-A$ to $+A$ the initial conditions are $u_r = u_r(0) = -A + r\Delta u$ and $u'_r = u'_r(0) = \sqrt{|2\int_A^{u_r} -f(u)du|}$; the other parameters are calculated as:

$$\Phi_{rs} = \begin{cases} -0.5\pi & \text{if } u'_r = 0 \\ \tan^{-1}[\omega_{rs}(u_r - C_{rs})/u'_r] & \text{if } u'_r < 0 \end{cases} \tag{3.11}$$

and

$$\Delta T = \begin{cases} (0.5\pi - \Phi_{rs})/\omega_{rs} & \text{if } (u_s - C_{rs}) \geq R_{rs} \\ (0.5\pi - \cos^{-1}[(u_s - C_{rs})/R_{rs}] - \Phi_{rs})/\omega_{rs} & \text{if } (u_s - C_{rs}) < R_{rs} \end{cases} \tag{3.12}$$

At the end of each discretization, we have $T_s = T_r + \Delta T$, and the end conditions u_s and u'_s are calculated by replacing r with s in the formulae for initial conditions.

3.2 Solution for negative linearized stiffness

When the sign in equation (12) is negative, the solution is:

$$u(T) = A_{rs}\exp(\omega_{rs}(T - T_r)) + B_{rs}\exp(-\omega_{rs}(T - T_r)) + C_{rs} \tag{3.13}$$

which can be expressed in the fractional time as:

$$u(t) = A_{rs}\exp\left(\frac{\omega_{rs}}{\Gamma(1+\alpha)}(t^\alpha - t_r^\alpha)\right) + B_{rs}\exp\left(-\frac{\omega_{rs}}{\Gamma(1+\alpha)}(t^\alpha - t_r^\alpha)\right) + C_{rs} \tag{3.14}$$

where $\omega_{rs} = \sqrt{K_{rs}}$ and $C_{rs} = u_r - F_r/K_{rs}$. The initial and end conditions are determined in the same as in Section 3.1. The integration constants are obtained by applying the initial conditions to get: $A_{rs} = \frac{1}{2}(u_r + u'_r/\omega_{rs} - C_rs)$ and $B_{rs} = \frac{1}{2}(u_r - u'_r/\omega_{rs} - C_rs)$. Then, using the end conditions in equation (3.13), we get:

$$\Delta T = \begin{cases} \frac{1}{\omega_{rs}}\log_e\left[\frac{(u_s - C_{rs}) \pm \sqrt{(u_s - C_{rs})^2 - 4A_{rs}B_{rs}}}{2A_{rs}}\right] & \text{if } (u_s - C_{rs}) > \sqrt{2A_{rs}B_{rs}} \\ \frac{1}{\omega_{rs}}\log_e\left(\frac{u_s - C_{rs}}{2A_{rs}}\right) & \text{if } (u_s - C_{rs}) \leq \sqrt{2A_{rs}B_{rs}} \end{cases} \tag{3.15}$$

The sign before the square root in equation (3.15) is negative for the oscillation stage that moves from $+A$ to $-A$ and vice versa. Note that if $u'_r = 0$, then $A_{rs} = B_{rs} = \frac{1}{2}(u_r - C_{rs})$ and

$$u(t) = (u_s - C_{rs})\cosh\left(\frac{\omega_{rs}}{\Gamma(1+\alpha)}(t^\alpha - t_r^\alpha)\right) + C_{rs} \tag{3.16}$$

3.3 Solution for zero linearized stiffness

In rare occurrence, we may have $K_{rs} = 0$ for a couple of discretization. This may happen for very large n and can be eliminated by increasing or decreasing n slightly. However, to account for $K_{rs} = 0$ we have:

$$u(T) = H_{rs} + G_{rs}(T - T_r) - \frac{1}{2}F_r(T - T_r)^2 \tag{3.17}$$

which can be expressed in fractional time as:

$$u(t) = H_{rs} + \frac{G_{rs}}{\Gamma(1+\alpha)}(t^\alpha - t_r^\alpha) - \frac{F_r}{2[\Gamma(1+\alpha)]^2}(t^\alpha - t_r^\alpha)^2 \tag{3.18}$$

where $G_{rs} = u'_r + F_r T_r$; $H_{rs} = u_r - u'_r T_r - \frac{1}{2}F_r T_r^2$ and

$$\Delta T = \frac{G_{rs} + \sqrt{G_{rs}^2 + 2F_r(H_{rs} - u_s)}}{F_r} \tag{3.19}$$

3.4 Implementation of CPLM solution for fractional oscillators

A pseudocode algorithm that summarizes the CPLM solution for fractional-order oscillators and that can be used to develop a computer code to implement the CPLM is provided in the appendix. For any fractional-order oscillator, the main CPLM parameters are K_{rs}, u'_r and C_{rs}. The other parameters depend on these three parameters and the initial/end conditions. The solution can be implemented for $n \geq 1$ but the accuracy of the solution depends on the number of discretization. This implies an apparent question as to how many discretization is needed to give the required accuracy. There is no known quantitative method to determine this but experience from previous studies [3, 9] shows that $n = 25$ gives a relative error that is less than 0.1% in most cases while for some oscillators with complex nonlinear restoring force [9], $n \geq 100$ would be needed to get the required accuracy.

4 Results and discussions

To demonstrate the effectiveness and accuracy of the CPLM algorithm to estimate the response of nonlinear fractional-order oscillators, typical instances of fractional-order oscillators that are relevant in engineering and physics were investigated in this section. The CPLM solutions for these oscillators were obtained for $n \geq 10$ and verified using exact solutions. The investigations presented in this section are for $0 < \alpha \leq 1.0$.

4.1 Fractional Duffing oscillator

The fractional Duffing oscillator arises in microphysics and tsunami motion [30]. Also, it has been used to study a jump phenomenon that is not possible with the classical Duffing oscillator [25]. The model for the fractional Duffing oscillator is given as [30]:

$$\frac{d^2u}{dt^{2\alpha}} + k_1 u + k_3 u^3 = 0 \tag{4.1}$$

The initial conditions are $u(0) = A$ and $D^\alpha u(0) = 0$. Application of the HFT results in:

$$\frac{d^2u}{dT^2} + k_1 u + k_3 u^3 = 0 \tag{4.2}$$

with initial conditions $u(0) = A$ and $u'(0) = 0$. Therefore, $f(u) = k_1 u + k_3 u^3$. The CPLM parameters necessary to obtain an approximate solution were derived as:

$$K_{rs} = k_1 + k_3(u_s^2 + u_s u_r + u_r^2) \tag{4.3a}$$

$$u'_r = \pm\left[k_1(A^2 - u_r^2) + \frac{1}{2}k_3(A^4 - u_r^4)\right] \tag{4.3b}$$

$$C_{rs} = u_r\left[1 - \frac{k_1 + k_3 u_r^2}{k_1 + k_3(u_s^2 + u_s u_r + u_r^2)}\right] \tag{4.3c}$$

All the other parameters can be calculated based on these three parameters.

On the other hand, the exact solution to the classical Duffing oscillator in equation (4.2) is given in terms of the Jacobi cosine function as shown [5]:

$$u(T) = Acn(\Psi T; m) \tag{4.4}$$

where $\Psi = \sqrt{k_1 + k_3 A^2}$ and $m = (k_3 A^2)/[2(k_1 + k_3 A^2)]$. Consequently, the exact solution to the fractional Duffing oscillator is:

$$u(t) = Acn\left(\frac{\sqrt{k_1 + k_3 A^2}}{\Gamma(1+\alpha)} t^{\alpha}; \frac{k_3 A^2}{2(k_1 + k_3 A^2)}\right) \tag{4.5}$$

Results of the CPLM solution and exact solution (equation (4.5)) for the fractional Duffing oscillator are shown in Figures 2 to 5. The agreement between the both solutions is excellent and the maximum error of the CPLM solution was found to be less than 0.05 % for $n = 10$. In contrast, the solution derived in ref. [30] using the amplitude-frequency formulation was found to produce up to 7.0 % error at large amplitudes. Each of the figures show solutions for $\alpha = 0.5$ and $\alpha = 1$ and it was observed that the fractional-order parameter introduces aperiodicity and an-harmonicity to the oscillations, with each successive cycle taking a longer time to complete. However, the ratio of the time taken to complete the $(j+1)^{th}$ cycle to the time taken to complete the j^{th} cycle decreases as time progresses and approaches unity as $j \to \infty$ where $j \in \mathbb{N}$. In contrast, the integer-order oscillator ($\alpha = 1$) completes each cycle at a fixed time which is known as the time period. In order words, the fractional-order oscillator has no time period.

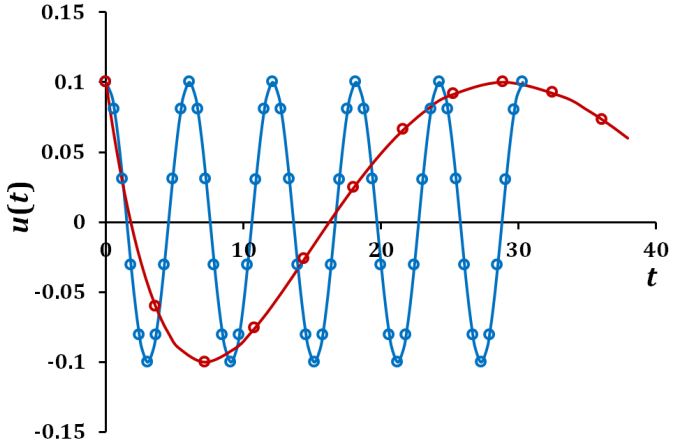

Figure 2: Small-amplitude oscillations ($A = 0.10$) of a fractional Duffing oscillator for $k_1/k_3 < 1$. Color representation: blue ($\alpha = 1.0$) and brown ($\alpha = 0.50$). Line (CPLM solution) and circle marker (Exact solution).

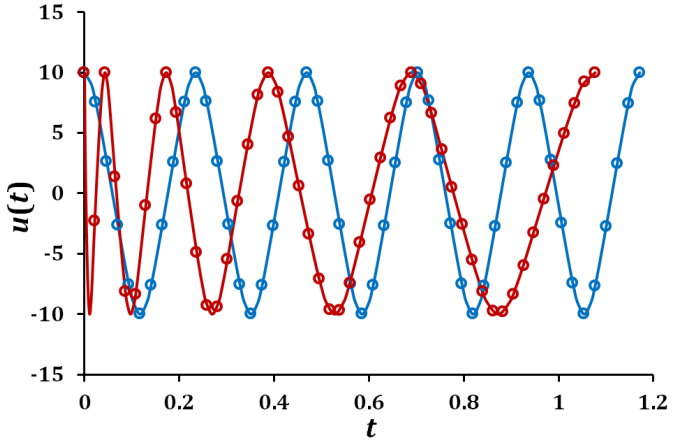

Figure 3: Large-amplitude oscillations ($A = 10.0$) of a fractional Duffing oscillator for $k_1/k_3 < 1$. Legend is the same as Figure 2.

The small- and large-amplitude oscillations of the fractional Duffing oscillator were investigated for two cases: (a) weak static nonlinearity ($k_1/k_3 = 0.1 < 1$) and (b) strong static nonlinearity ($k_1/k_3 = 10 > 1$). The responses for the case of weak static nonlinearity are shown in Figures 2 and 3, while Figures 4 and 5 are for strong static nonlinearity. The figures reveal that increasing the amplitude leads to an increase in the number of cycles that can be completed in

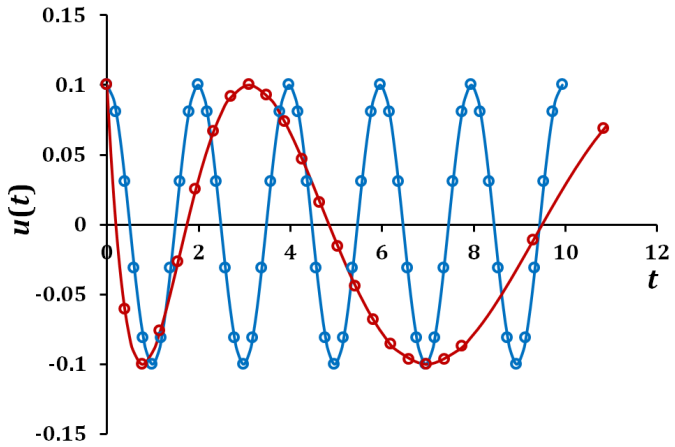

Figure 4: Small-amplitude oscillations ($A = 0.10$) of a fractional Duffing oscillator for $k_1/k_3 > 1$. Legend is the same as Figure 2.

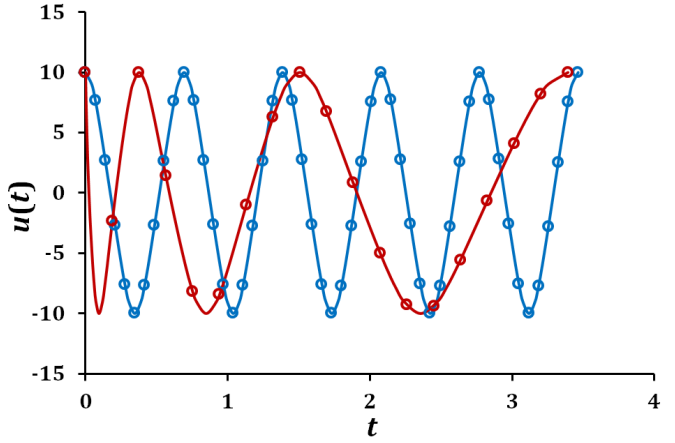

Figure 5: Large-amplitude oscillations ($A = 10.0$) of a fractional Duffing oscillator for $k_1/k_3 > 1$.

a given time. This is consistent with the behavior of the Duffing oscillator which is known to increase its frequency (or decrease its time period) with increase in amplitude. The system with weak static nonlinearity appeared to be more sensitivity to the amplitude compared to the system with strong static nonlinearity. This happens because the strong static nonlinearity produces a counteracting resilience to the flexibility of the oscillator, thereby giving rise to a more gradual change in the nonlinear response as the amplitude changes. Hence, the system with weak static nonlinearity is more sensitive to changes in the fractional-order parameter.

4.2 Fractional pendulum

Pendulum-like motions occur in a number of systems including acoustic vibrations, molecular oscillations, optically torqued nanorods, elliptic filters and quantum oscillators [23]. At the microscopic and quantum scale, the pendulum-like oscillations can be better described by the fractional differential equation in equation (4.6).

$$\frac{d^2u}{dt^{2\alpha}} + \omega_0^2 \sin u = 0 \tag{4.6}$$

where u is the angular displacement and ω_0 is a constant that depends on the system's properties. The initial conditions for the fractional pendulum are given as $u(0) = A$ and $D^\alpha u(0) = 0$. Applying the HFT gives the equivalent continuous model as:

$$\frac{d^2u}{dT^2} + \omega_0^2 \sin u = 0 \tag{4.7}$$

with initial conditions $u(0) = A$ and $u'(0) = 0$. Then, the restoring force is $f(u) = \omega_0^2 \sin u$ and the main CPLM parameters were derived as:

$$K_{rs} = \frac{\omega_0^2(\sin u_s - \sin u_r)}{u_s - u_r} \tag{4.8a}$$

$$u_r' = \pm\omega_0^2\sqrt{2(\cos u_r - \cos u_s)} \tag{4.8b}$$

$$C_{rs} = u_r - \frac{(u_s - u_r)\sin u_r}{(\sin u_s - \sin u_r)} \tag{4.8c}$$

The exact solution to equation (33) can be derived as shown [23]:

$$u(T) = 2\sin^{-1}[ksn(\omega_0 T + K(k^2); k^2)] \tag{4.9}$$

where sn is the Jacobi elliptic sine function, $k = \sin(A/2)$ and $K(k^2)$ is the complete elliptic integral of the first kind given as:

$$K(k^2) = \int_0^{\pi/2} \frac{1}{\sqrt{1 - k^2\sin^2\phi}} d\phi \tag{4.10}$$

From equations (9) and (35), the exact solution to the fractional pendulum oscillations is:

$$u(t) = 2\sin^{-1}\left[\sin\left(\frac{A}{2}\right) sn\left(\frac{\omega_0}{\Gamma(1+\alpha)}t^\alpha + K\left(\sin^2\left(\frac{A}{2}\right)\right); \sin^2\left(\frac{A}{2}\right)\right)\right]. \tag{4.11}$$

Figures 6 to 8 shows the response of the fractional pendulum for $\alpha = (0.5, 0.75, 1)$ obtained using the CPLM and exact solution. The CPLM results are seen to match the exact result and the maximum error of the CPLM solution was found to be less than 0.2 % for $n = 100$. Small-amplitude (Figure 6), moderate-amplitude (Figure 7) and large-amplitude (Figure 8) responses were simulated. It was observed that a decrease in the value of the fractional-order parameter increased the aperiodic and an-harmonic behavior of the response, and increased the time taken to complete a cycle. In contrast to the fractional Duffing oscillator, the fractional pendulum response shows a decrease in the number of cycles completed in a given time as the amplitude increases. This can be explained by the fact that the static nonlinearity, which arises due to geometric effect, increases in strength as the amplitude increases. This nonlinearity produces a softening effect that slows the pendulum at larger amplitudes. As the pendulum becomes slower, it completes fewer cycles in a given time. It was observed that while the time taken to complete each cycle is constant for $\alpha = 1$, the time taken to complete a cycle increases for successive cycles when $0 < \alpha < 1$. Also, the change in time required from one cycle to the next increases as α decreases.

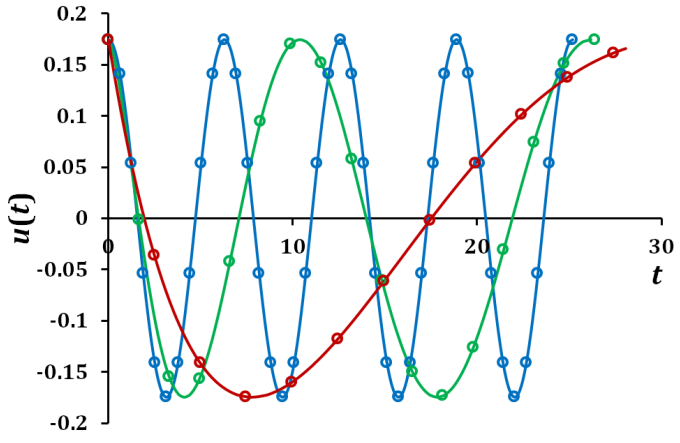

Figure 6: Small-amplitude oscillations ($A = 10°$) of a fractional pendulum for different values of the fractional parameter. Color representation: blue ($\alpha = 1.0$), green ($\alpha = 0.75$) and brown ($\alpha = 0.50$). Line (CPLM solution) and circle marker (Exact solution).

4.3 Fractional Mathews-Lakshmanan oscillator

The Mathews-Lakshmanan oscillator [27] describes the motion of elementary particles in a relativistic scalar field. It was derived from the Lagrangian of elementary particle theory of pion interactions. An interesting feature of

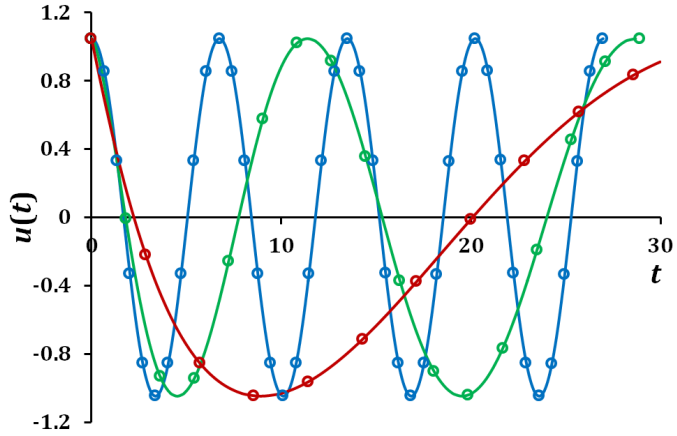

Figure 7: Moderate-amplitude amplitude oscillations ($A = 60°$) of a fractional pendulum for different values of the fractional parameter. Legend is the same as Figure 6.

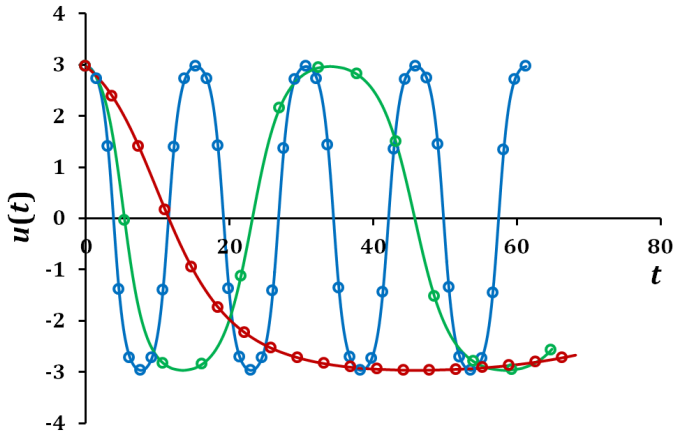

Figure 8: Large-amplitude oscillation ($A = 170°$) of the fractional Mathews-Lakshmanan oscillator for different values of the fractional parameter. Legend is the same as Figure 6.

the Mathews-Lakshmanan oscillator is that all its bounded periodic motions are simple harmonic even though it is a nonlinear oscillator. It is understood from quantum mechanics that elementary particle motion is discontinuous. Therefore, a fractional Mathews-Lakshmanan oscillator is considered to describe the pion interactions. The model for the fractional oscillator is:

$$(1+\lambda u^2)\frac{d^2u}{dt^{2\alpha}} + \lambda u\left(\frac{du}{dt^{\alpha}}\right)^2 + \Lambda u = 0 \tag{4.12}$$

where $u(0) = A$ and $D^{\alpha}u(0) = 0$ are the initial condition. Applying the HFT gives the equivalent integer-order oscillator as:

$$(1+\lambda u^2)\frac{d^2u}{dT^2} + \lambda u\left(\frac{du}{dT}\right)^2 + \Lambda u = 0 \tag{4.13}$$

where the initial conditions are $u(0) = A$ and $u'(0) = 0$. Ref [29] showed that for an oscillator in the form:

$$I(u)\frac{d^2u}{dT^2} + \frac{dI}{du}\left(\frac{du}{dT}\right)^2 = Q(u) \tag{4.14}$$

the velocity and restoring force can be derived from:

$$\frac{du}{dT} = \pm\sqrt{\frac{2[h(A)-h(u)]}{[I(u)]^{2k}}} \tag{4.15}$$

and

$$f(u) = \frac{2k\frac{dI}{du}[h(A) - h(u)]}{[I(u)]^{2k+1}} - \frac{Q(u)}{I(u)} \tag{4.16}$$

where

$$h(u) = -\int [I(u)]^{2k-1} Q(u) du \tag{4.17}$$

From equation (39), $I(u) = 1 + \lambda u^2$, $Q(u) = -\Lambda u$ and $k = -1/2$. Therefore,

$$\frac{du}{dT} = \pm\Lambda^{-1/2}\sqrt{\frac{A^2 - u^2}{1 + \lambda A^2}} \tag{4.18}$$

from which we get:

$$T = \left(\frac{\Lambda}{1 + \lambda A^2}\right)^{1/2} \int_u^A \frac{dy}{\sqrt{A^2 - y^2}} \tag{4.19}$$

Now, using the transformation $y = A\cos\theta$, the solution to equation (4.19) can be derived as:

$$u(T) = A\cos\left(\left[\frac{\Lambda}{1 + \lambda A^2}\right]^{1/2} T\right) \tag{4.20}$$

Equation (4.20) is the exact solution of the continuous Mathews-Lakshmanan oscillator and it is a simple harmonic solution. The exact solution of the fractional Mathews-Lakshmanan oscillator is obtained from equations (3.2) and (4.20) as:

$$u(T) = A\cos\left(\frac{1}{\Gamma(1+\alpha)}\sqrt{\frac{\Lambda}{1 + \lambda A^2}}\, t^\alpha\right) \tag{4.21}$$

In order to apply the CPLM solution to derive the periodic solution of the fractional Mathews-Lakshmanan oscillator, we need to know the restoring force which was determined from equation (4.16) to be $f(u) = \Lambda u/(1 + \lambda A^2)$. Then, the main CPLM constants were derived as:

$$K_{rs} = \Lambda/(1 + \lambda A^2) \tag{4.22a}$$

$$u_r' = \pm\Lambda^{-1/2}\sqrt{\frac{A^2 - u_r^2}{1 + \lambda A^2}} \tag{4.22b}$$

$$C_{rs} = 0 \tag{4.22c}$$

By virtue of the fact that $f(u) = \Lambda u/(1+\lambda A^2)$ is linear, we know that the solution must be a simple harmonic motion. In this case, we implement the CPLM solution for $n = 1$ because K_{rs} is constant for any number of discretization. This implies that $t_r = 0$, $u_r = A$, $u_s = 0$, $u_r' = 0$, $R_{rs} = A$, $\omega_{rs} = \sqrt{\Lambda/(1 + \lambda A^2)}$, and $\Phi_{rs} = \pi/2$. Substituting these results in equation (3.8) gives the CPLM solution for the fractional Mathews-Lakshmanan oscillator as:

$$u(t) = A\sin\left(\frac{\pi}{2} + \frac{1}{\Gamma(1+\alpha)}\sqrt{\frac{\Lambda}{1 + \lambda A^2}}\, t^\alpha\right) \tag{4.23}$$

which is the same as the exact solution in equation (4.21). This means that a single iteration of the CPLM algorithm, which is easily done by manual computation, gave the exact solution of the fractional Mathews-Lakshmanan oscillator. Based on the derived restoring force, the Mathews-Lakshmanan oscillator can be expressed as an equivalent linear oscillator as follows:

$$\frac{d^2u}{dT^2} + \frac{\Lambda}{1 + \lambda A^2}u = 0 \tag{4.24}$$

where the amplitude-dependent frequency originates from the nonlinearity in the system. The response of the fractional Mathews-Lakshmanan oscillator for small- and large-amplitude oscillations were simulated in Figures 9 and 10 respectively. The figures show the CPLM and exact solutions, both of which give the same results. The effects of the fractional-order parameter and amplitude on the oscillation are the same as found in the fractional Duffing oscillator. For the integer-order oscillation (i.e. $\alpha = 1$), the response was found to be purely simple harmonic, but with an amplitude-dependent frequency (see equation (4.24)).This explains why the time period for Figure 9 is different from Figure 10 even though the periodic response of the Mathews-Lakshmanan oscillator has an equivalent linear oscillator representation. Finally, the fractional Mathews-Lakshmanan oscillator produced strong nonlinear characteristics such as an-harmonic and aperiodic response despite the fact that the integer-order Mathews-Lakshmanan oscillator produces linear response characteristics.

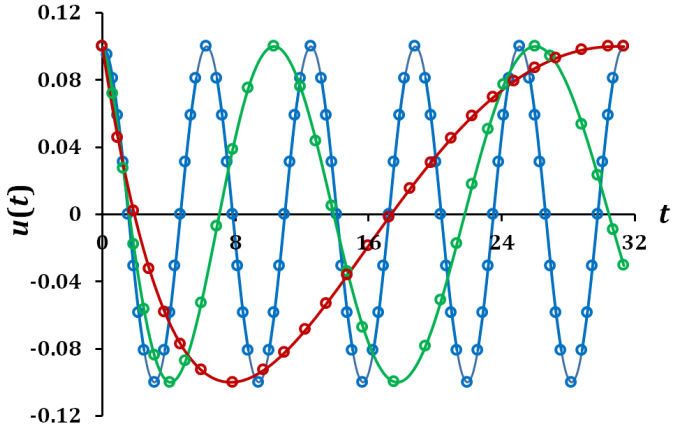

Figure 9: Small-amplitude oscillations ($A = 0.10$) of the fractional Mathews-Lakshmanan oscillator for different values of the fractional parameter. Legend is the same as Figure 6.

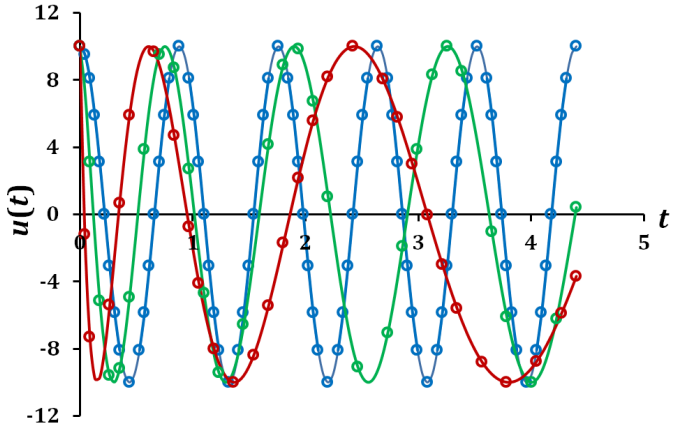

Figure 10: Large-amplitude oscillation ($A = 10$) of the fractional Mathews-Lakshmanan oscillator for different values of the fractional parameter. Legend is the same as Figure 6.

5 Conclusions

This paper provides an accurate method for the approximate solution of nonlinear fractional oscillators. These oscillators are characterized by a second-order fractional derivative and a nonlinear restoring force. The fractional derivative was defined by a modified Riemann-Liouville derivative that is suitable for initial-value problems. The fractional-order model was transformed into an equivalent continuous model by means of the He fractional transform. The continuous model was then solved by the continuous piecewise linearization method, from which the solution of the nonlinear fractional oscillator was obtained. In order to demonstrate the CPLM solution, typical nonlinear fractional oscillators were investigated and the CPLM solutions were verified using exact solutions. It was observed that the error of the CPLM algorithm was negligible and in the case of the fractional Mathews-Lakshmanan oscillator, the CPLM algorithm produced an exact solution.

The results simulated produced some interesting observations. First, the fractional-order parameter introduces aperiodicity and an-harmonicity to the oscillations, with each successive cycle taking a longer time to complete. Secondly, the ratio of the time taken to complete the $(j+1)^{th}$ cycle to the time taken to complete the j^{th} cycle of a fractional oscillator decreases as time progresses and approaches unity as $j \to \infty$. Thirdly, a fractional oscillator with a hardening and weak static nonlinearity is more sensitive to changes in the fractional-order parameter compared to one with strong static nonlinearity. Fourthly, the time taken to complete a cycle increases as the fractional-order parameter moves away from 1 towards zero. However, when the fractional-order parameter is very close to zero, the response can be said to be static. Fifthly, the fractional oscillator is nonlinear even though its equivalent continuous or integer-order oscillator is linear. Therefore, the fractional-order parameter provides an additional variable that can be used to study nonlinear responses that cannot be predicted by integer-order oscillators ($\alpha = 1$) e.g. noise attenuation

in a vibrating system [30] or non-periodic oscillations. The CPLM algorithm provides an accurate tool for the study of such nonlinear fractional oscillators.

References

[1] A. Atangana and J.F. Gomez-Aguilar, *Numerical approximation of Riemann-Liouville definition of fractional derivative: From Riemann-Liouville to Atangana-Baleanu*, Numer. Methods Partial Differential Eq. **36** (2017), no. 4, 1502–1523.

[2] A. Atangana and J.F. Gomez-Aguilar, *Decolonisation of fractional calculus rules: Breaking commutativity and associativity to capture more natural phenomena*, Eur. Phys. J. Plus **133** (2018), 166–187.

[3] A. Big-Alabo, *Periodic solutions of Duffing-type oscillators using continuous piecewise linearization method*, Mech. Eng. Res. **8** (2018), no. 1, 41–52.

[4] A. Big-Alabo, *Approximate periodic solution and qualitative analysis of non-natural oscillators based on the restoring force*, Eng. Res. Exp. **2** (2020), no. 1, 015029. 14 pp.

[5] A. Big-Alabo, *A simple cubication method for approximate solution nonlinear Hamiltonian oscillators*, Int'l J. Mech. Eng. Educ. **48** (2020), no. 3, 241–254.

[6] A. Big-Alabo, *Continuous piecewise linearization method for approximate periodic solution of the relativistic oscillator*, Int'l J. Mech. Eng. Educ. **48** (2020), no. 2, 178–194.

[7] A. Big-Alabo, P. Harrison and M.P. Cartmell, *Algorithm for the solution of elastoplastic half-space impact: force-indentation linearisation method*, Proc. IMechE, C: J. Mech. Eng. Sci. **229** (2015), no. 5, 850–858.

[8] A. Big-Alabo, C.O. Ogbodo and C.V. Ossia, *Semi-analytical treatment of complex nonlinear oscillations arising in the slider-crank mechanism*, World Sci. News **142** (2020), 1–24.

[9] A. Big-Alabo and C.V. Ossia, *Periodic Solution of Nonlinear Conservative Systems*, Progress in Relativity, 2020.

[10] M. Caputo and M. Fabrizio, *A new definition of fractional derivative without singular kernel*, Progr. Fract. Differ. Appl. **1** (2015), 73-–85.

[11] M. Di Paola and M. Zingales , *Exact mechanical models of fractional hereditary materials*, J. Rheol. **56** (2012), no. 5, 983–1004.

[12] R. Garrappa, *Grünwald–Letnikov operators for fractional relaxation in Havriliak-Negami models*, Commun. Nonlinear Sci. Numer. Simulat. **38** (2016), 178-–191.

[13] J,F. Gomez-Aguilar, H. Yépez-Martínez, C. Calderón-Ramón, I. Cruz-Orduña, R.F. Escobar-Jiménez and V.H. Olivares-Peregrino, *odeling of a Mass-Spring-Damper System by Fractional Derivatives with and without a Singular Kernel*, Entropy **17** (2015), 6289–6303.

[14] J.H. He, *Approximate analytical solution for seepage flow with fractional derivatives in porous media*, Comput. Meth. Appl. Mech. Eng. **167** (1998), 57—68.

[15] J.H. He, *A new fractal derivation*, Therm. Sci. **15** (2011), 145—147.

[16] J.H. He, *Asymptotic methods for Solitary Solutions and Compactons*, Abstr. Appl. Anal. **2012** (2012), Article ID: 916793, 1–130.

[17] J.H. He, *A tutorial review on fractal spacetime and fractional calculus*, Int. J. Theor. Phys. **53** (2014), 3698—3718.

[18] J.H. He, *Fractal calculus and its geometrical explanation*, Results Phys. **10** (2018), 272–276.

[19] G. Jumarie, *Modified Riemann-Liouville Derivative and Fractional Taylor Series of Non-differentiable Functions Further Results*, Comp. Math. Appl. **51** (2006), 1137—1376.

[20] U.N. Katugampola, *New approach to a generalized fractional integral*, Appl. Math. Comp. **218** (2011), no. 3, 860–865.

[21] U.N. Katugampola, *A new approach to generalized fractional derivatives*, Bul. Math. Anal. Appl. **6** (2014), no. 4, 1–15.

[22] R. Khalil, M. Al Horani, A. Yousef and M. Sababheh, *A new definition of fractional derivative*,J. Comput. Appl. Math. **264** (2014), 65–70.

[23] F.M.S. Lima, *Simple but accurate periodic solutions for the nonlinear pendulum equation*, Rev. Bras. Ens. Fís. **41** (2019), no. 1, e20180202-1-6.

[24] Y. Liu, Y.W. Du, H. Li and J.F. Wang, *A two-grid finite element approximation for a nonlinear time-fractional Cable equation*, Phys. Lett. A **85** (2016), 2535-–2548.

[25] Q.X. Liu, J.K. Liu and Y.M. Chen, *An analytical criterion for jump phenomena in fractional Duffing oscillators*, Chaos, Solits. Fractals **98** (2017), 216—219.

[26] Y. Luchko, *A new fractional calculus model for the two-dimensional anomalous diffusion and its analysis*, Math. Model. Nat. Phenom. **11** (2017), no. 3, 1—17.

[27] P.M. Mathews and M. Lakshmanan, *On a unique nonlinear oscillator*, Q. Appl. Math. **32** (1974), 215—218.

[28] S. Momani and Z. Odibat, *Homotopy perturbation method for nonlinear partial differential equations of fractional order*, Eur. Phys. J. Plus **365** (2007), 345-–350.

[29] V.F. Morales-Delgado, J.F. Gomez-Aguilar, K.M. Saad, M.A. Khan and P. Agarwal, *Analytic solution for oxygen diffusion from capillary to tissues involving external force effects: A fractional calculus approach*, Phys. A **523** (2019), 48–65.

[30] Y. Wang and J.Y. An, *Amplitude–frequency relationship to a fractional Duffing oscillator arising in microphysics and tsunami motion*, J. Low Freq. Noise Vib. Active Control **38** (2019), no. 3-4, 1008–1012.

[31] Y. Wang, Y.F. Zhang and W.J. Rui, *Shallow water waves in porous medium for coast protection*, Therm. Sci. **21** (2017), 145-–151.

[32] X.J. Yang, *General Fractional Derivatives - Theory, Methods and Applications*, CRC Press, Taylor and Francis Group, Boca Raton, 2019.

[33] X.J. Yang and D. Baleanu, *Fractal heat conduction problem solved by local fractional variational iteration method*, Therm. Sci. **17** (2013), no. 2, 625–628.

Appendix A Pseudocode algorithm for implementing the CPLM solution to nonlinear fractional-order oscillators

START

$\Delta u = A/n$ **Displacement increment for each discretization**

GET(A, n, α and other parameters of the oscillator) **Input values**

$r = 0$; PUT (0, ",", A) **Initialize r and print initial solution**

IF ($A > 0$) THEN **$A > 0$ implies negative velocity oscillation stage**

DO UNTIL ($r = 2n$)

$u_r = A - r\Delta u$; $u'_r = -\sqrt{|2\int_A^{u_r} -f(u)du|}$ **Initial conditions**

$s = r + 1$; $u_s = A - s\Delta u$; $u'_s = -\sqrt{|2\int_A^{u_s} -f(u)du|}$ **End conditions**

$K_{rs} = [f(u_s) - f(u_r)]/(u_s - u_r)$; **Linearized stiffness**

IF ($K_{rs} > 0$) THEN

$\omega_{rs} = \sqrt{K_{rs}}$; $C_rs = u_r - F_r/K_{rs}$; $R_{rs} = [(u_r - C_{rs})^2 + (u'_r/\omega_{rs})^2]^{1/2}$;

IF ($u'_r = 0$) THEN

$\Phi_{rs} = 0.5\pi$;

ELSEIF ($u'_r < 0$) THEN

$\Phi_{rs} = \pi + \tan^{-1}[\omega_{rs}(u_r - C_{rs})/u'_r]$;

END_ELSEIF

IF $((u_s - C_{rs}) \geq R_{rs})$ THEN

$\Delta T = (0.5\pi - \Phi_{rs})/\omega_{rs}$;

ELSEIF $((u_s - C_{rs}) < R_{rs})$ THEN

$\Delta T = (0.5\pi + \cos^{-1}[(u_s - C_{rs})/R_{rs}] - \Phi_{rs})/\omega_{rs}$;

END_ELSEIF

$T_s = T_r + \Delta T$; $t_s = (T_s \Gamma(1+\alpha))^{1/\alpha}$; **Continuous and fractal time at end point**

$u(t) = R_{rs} \sin\left(\frac{\omega_{rs}}{\Gamma(1+\alpha)}(t^\alpha - t_r^\alpha) + \Phi_{rs}\right) + C_{rs}$;

ELSEIF $(K_{rs} < 0)$ THEN

$\omega_{rs} = \sqrt{K_{rs}}$; $A_{rs} = \frac{1}{2}(u_r + u_r'/\omega_{rs} - C_r s)$; $B_{rs} = \frac{1}{2}(u_r - u_r'/\omega_{rs} - C_r s)$;

$\Delta T = \frac{1}{\omega_{rs}} \log_e \left[\frac{(u_s - C_{rs}) \pm \sqrt{(u_s - C_{rs})^2 - 4A_{rs}B_{rs}}}{2A_{rs}}\right]$;

$T_s = T_r + \Delta T$; $t_s = (T_s \Gamma(1+\alpha))^{1/\alpha}$;

$u(t) = A_{rs} \exp\left(\frac{\omega_{rs}}{\Gamma(1+\alpha)}(t^\alpha - t_r^\alpha)\right) + B_{rs} \exp\left(-\frac{\omega_{rs}}{\Gamma(1+\alpha)}(t^\alpha - t_r^\alpha)\right) + C_{rs}$;

END_ELSEIF

PUT (t_s, ",", u_s) **Prints the time and displacement at end condition**

$r = s$; $u_r = u_s$; $u_r' = u_s'$; **Update initial conditions for the next discretization**

END_DO

END_THEN

STOP

The pseudocode algorithm above is for the first half cycle of the continuous model (i.e. from $+A$ to $-A$). A similar algorithm is applicable for the second half and the necessary changes can be seen in Section 3. This pseudocode algorithm was applied to develop a Mathematica program to implement the CPLM solution. Note that the solution $u(t)$ is only used if data points are extracted from each discretization to get sufficient points to make a smooth plot. However, for $n \geq 25$, extracting data points from each discretization is unnecessary, and the end conditions give sufficient points to produce a smooth plot.